

RF shimming in human torso with the multi-mode coaxial waveguide at 7T

Anna Andreychenko¹, Vincent O. Boer¹, Jan J.W. Lagendijk¹, Peter R. Luijten¹, and Cornelis A.T. van den Berg¹
¹Imaging Division, UMC Utrecht, Utrecht, Netherlands

Introduction: Volume coils are attractive RF transmit systems as they provide flexible means of RF excitation for the whole body. The performance of classical volume coils at ultra high field is strongly degraded by the waveguide action of the RF shield [1]. Recently, a coaxial waveguide concept as a candidate for a whole body RF transmitter was presented [2]. By adding dielectric lining to the RF shield, multiple travelling wave modes become above cut off. This presence of multiple travelling wave modes provides diverse excitation patterns in transverse plane and more importantly in the longitudinal direction. This allows for a good RF shimming performance at 7T in the human head [3]. The same setup could be used for 3D RF shimming on specific body sites. Here the transmit performance of the multi-mode coaxial waveguide for a few anatomical sites of body torso was investigated in terms of the achieved B_1^+ efficiency, homogeneity and RF safety constraints.

Methods: The male human model from the Virtual Family [4] was placed in the multi-mode coaxial waveguide [3] with his legs in the coaxial waveguide (Fig. 1). The multi-mode coaxial waveguide had 8 individually fed antennas. EM field distributions of each antenna in the body torso were simulated using the FDTD method (SEMCAD, SPEAG, Zurich, Switzerland). The following body sites were chosen for RF shimming: liver, kidneys and prostate. Optimization of the phase setting of individual channels B_1^+ maps was performed with an in-house developed B_1^+ shimming tool (MATLAB 7.5, The MathWorks Inc., Natick, MA, 2007). Only B_1^+ phase shimming was performed as amplitude shimming leads generally to increased RF power levels [5]. Phase settings were calculated for RF shimming of the overall pelvis and of the separate body sites. Mean B_1^+ and standard deviation of B_1^+ were calculated in the selected body site. RF safety constraints were evaluated of the calculated phase settings in SEMCAD. B_1^+ efficiency and average SAR values are reported for 8x1kW delivered power. For MR experiments the multi-mode coaxial waveguide and a healthy volunteer were placed in the bore of a 7T MR scanner. Low FA GRE transverse images (amplitude and phase) (TE/TR=3/110 ms, acq. voxel: 5x5x5 mm³) were recorded in the body torso per antenna for five antennas. Based on a SVD approach, the relative transmit sensitivities were determined [6] which were subsequently used for the "off-line" RF shimming. As no dedicated receive array was available, the antennas were used in transmit and receive in the imaging experiments.

Results and discussion: FDTD simulated B_1^+ maps of individual channels are shown in Fig. 2. The optimal phase settings of each channel were calculated for RF shimming of the whole pelvis. The resulting 3D B_1^+ distribution in human torso was compared with the quadrature settings (Fig. 3). In the chosen region (outlined with the dashed line) the shimmed distribution had improved spatial homogeneity comparing to the quadrature, especially in AP and HF directions. However, standing wave effects were still present. 3D RF shimming on the three different targets in the body and consequent RF safety evaluation was performed. The results are summarized in Fig.4. A good shimming was achieved for a relatively large organ as liver. Remarkably, despite more distant location of liver from the coaxial waveguide edge than prostate, prostate and liver had the same B_1^+ efficiency. This is because the extension of dielectric lining over body torso effectively reduced attenuation of the wave propagating in body torso. Shimming of both kidneys appeared to be challenging but nonetheless, both of them could be excited with a similar efficiency as liver and prostate. The obtained in-vivo relative transmit sensitivities of five channels are present in Fig.5 A. The channels have distinct transmit sensitivities that could be exploited for RF shimming. Optimization of the phases was performed for the entire

A: Tx sensitivities of five channels

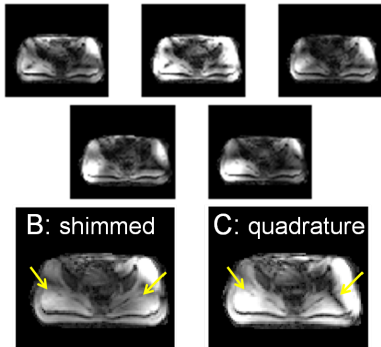


Figure 5: A: transverse Tx sensitivities of five channels, calculated based on the SVD method. Combined five channels with optimized (B) and quadrature (C) phase settings. Arrows point to the eliminated signal amplifications and voids with the optimized phase settings.

transverse slice. The shimmed image was compared to the quadrature channel combination (Fig.5 B&C). Overall a better image homogeneity was achieved with the optimized shim settings by eliminating undesirable signal amplification and void in the transverse plane (Fig.5 B&C, arrows). Image quality could be significantly improved if a dedicated local receive array was applied instead of the Tx/Rx antennas.

Conclusions: Provided large excitation coverage it was shown that the multi-mode coaxial waveguide could be applied for efficient overall and targeted 3D RF shimming in body torso.

References: [1] Vaughan JT et al. MRM 2009; [2] Andreychenko A et al. Proc. 19th ISMRM 2009; [3] Andreychenko A et al. Proc. 19th ISMRM 2011; [4] Christ A et al. Phys Med Biol 2010; [5] Van den Bergen B et al. JMRI 2009; [6] Brunner DO et al. Proc. 18th ISMRM 2010.

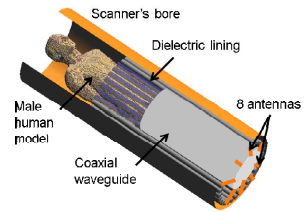


Figure 1. The multi-mode coaxial waveguide set-up for human torso MRI.

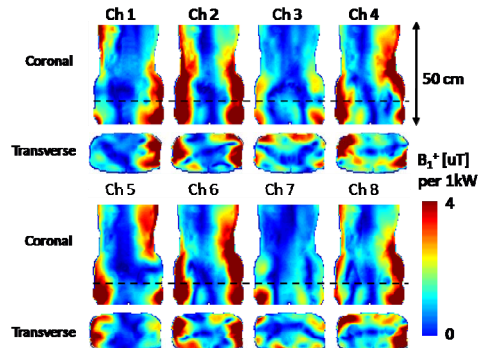


Figure 2. Individual coronal and transversal B_1^+ field distribution of eight channels. Location of the transversal slice is shown with dashed line.

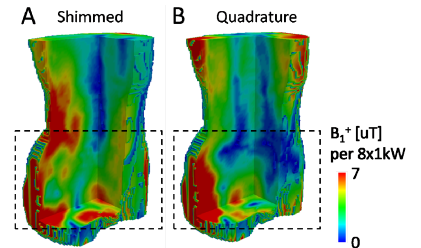


Figure 3. Eight channels' B_1^+ field distribution in male torso combined with the optimized (A) and quadrature (B) phase settings. The chosen region is outlined with dashed line.

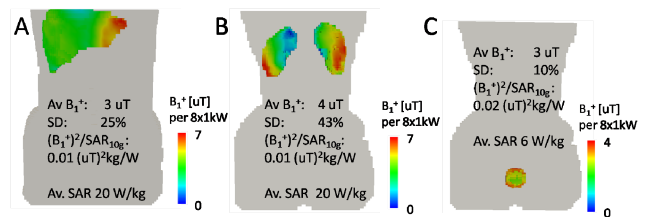


Figure 4. Combined eight channels' B_1^+ field distribution with phase settings optimized for liver (A), kidneys (B) and prostate (C) excitation. Body shape is depicted in grey. Average B_1^+ and standard deviation were calculated in the target 3D volume as well as the excitation efficiency over peak local SAR value and average SAR (per 8x1kW).